Research Square

Preprints are preliminary reports that have not undergone peer review.
They should not be considered conclusive, used to inform clinical practice,
or referenced by the media as validated information.

Neural stem cell-derived exosomes carrying lncRNA H19 and MEG3 are associated with neuronal-like differentiation of adipose-derived mesenchymal stem cells

Yosra Helalat
Shahid Chamran University of Ahvaz
Elham Hoveizi
e.hoveizi@yahoo.com
Shahid Chamran University of Ahvaz
Maryam Naderi-Soorki
Shahid Chamran University of Ahvaz

Article

Keywords: exosomes, neural differentiation, neural stem cells, long non-coding RNAs, nerve regeneration

Posted Date: November 25th, 2026

DOI: https://doi.org/10.21203/rs.3.rs-11641104/v1

License: This work is licensed under a Creative Commons Attribution 4.0 International License.
Read Full License

Additional Declarations: No competing interests reported.

Neural stem cell-derived exosomes carrying lncRNA H19 and MEG3 are associated with neuronal-like differentiation of adipose-derived mesenchymal stem cells

Yosra Helalat[1], Elham Hoveizi[1], Maryam Naderi-Soorki[1]

[1]Department of Biology, Faculty of Science, Shahid Chamran University of Ahvaz, Ahvaz, Iran

Correspondence to:

Elham Hoveizi
Department of biology, Faculty of Science, Shahid Chamran University of Ahvaz, Ahvaz, Iran

E-mail: e.hoveizi@scu.ac.ir & e.hoveizi@yahoo.com

Tel: 06133331045

ORCID: Elham Hoveizi: https://orcid.org/0000-0002-3285-5682

Running Title: NSCs Exosomal H19/MEG3 and Neuronal Differentiation

Abstract

Limited understanding of factors governing neural differentiation of stem cells has hindered neural tissue regeneration. This study examined exosomes derived from neural stem cells (NSCs-Exo) carrying long non-coding RNAs H19 and MEG3 as potential inducers for differentiating adipose-derived mesenchymal stem cells (ADMSCs) into neuronal-like cells (NLCs). Neural stem cells were enzymatically isolated from brains of one-day-old rat. Secreted exosomes were isolated using AnaCell chemical isolation kit and characterized by electron microscopy and Western blotting for exosomal markers. Presence of H19 and MEG3 lncRNAs inside exosomes was evaluated using RT-PCR. Uptake of DiI-labeled NSCs-Exo by ADMSCs was assessed by fluorescence microscopy, after which ADMSCs were exposed to NSCs-Exo. Neural differentiation was evaluated by analyzing expression of neural markers using RT-PCR and immunocytochemistry. Results showed successful isolation of NSCs-Exo with size range 30-100 nm and protein concentration 330.52 μg/mL. Labeled exosomes penetrated cell membrane and were internalized by ADMSCs. Exosomes contained both H19 and MEG3. Treatment significantly increased expression of neuronal markers including neurofilament (NF), MAP2, Nestin, and Tuj-1 compared with control group ($P \leq 0.001$). Findings indicate NSCs-Exo containing H19 and MEG3 are associated with enhanced neural differentiation of ADMSCs and may represent promising cell-free approach in regenerative medicine for neurological disorders.

Keywords: exosomes, neural differentiation, neural stem cells, long non-coding RNAs, nerve regeneration

Introduction

Neural stem cells (NSCs) are self-renewing and multipotent cells that are found in the central and peripheral nervous systems. During normal development, these cells are responsible for generating new neurons, astrocytes, and oligodendrocytes and therefore play a key role in the maintenance and repair of neural tissue [1,2]. In addition to their capacity for direct differentiation, NSCs exert effects on neighboring cells through the secretion of paracrine factors, including exosomes. Exosomes are small membrane-bound vesicles, approximately 30–150 nm in diameter, secreted by various cell types and functioning as natural carriers [3]. These vesicles contain a variety of biomolecules, including proteins, lipids, mRNAs, and long non-coding RNAs (lncRNAs), and participate in the regulation of various cellular processes by transferring this cargo to target cells [4].

NSC-derived exosomes (NSCs-Exo), owing to their neural origin, contain a rich repertoire of neurotrophic factors and regulatory RNAs and may enhance the differentiation of neural stem cells and neighboring cells toward a neural phenotype through modulation of signaling pathways [5,6]. Mesenchymal stem cells (MSCs) have also attracted considerable attention as potential tools in regenerative medicine and the treatment of neurodegenerative diseases because of their ability to differentiate into various mesodermal and non-mesodermal cell types, including neural cells [7]. However, induction of a neuronal-like phenotype in MSCs does not necessarily depend on classical direct differentiation. Recent evidence suggests that this process occurs predominantly through paracrine signals and the transfer of regulatory molecules by exosomes [8,9]. This approach has attracted considerable attention because of its simplicity and avoidance of direct genetic manipulation.

At the molecular level, lncRNAs are recognized as important regulators of neuronal differentiation. These regulatory molecules, which do not encode proteins, play a critical role in determining cell

fate by modulating gene expression at transcriptional, post-transcriptional, and epigenetic levels [10]. lncRNAs such as H19 and MEG3, following exosomal transfer, may interact with miRNAs, transcription factors, and downstream signaling pathways, thereby altering the balance between mesenchymal and neuronal phenotypes in target cells [11,12].

H19 is one of the best-characterized imprinted lncRNAs and has diverse roles in biological processes. Through regulation of the Wnt/β-catenin and PI3K/AKT pathways, H19 acts as an important regulator of neural cell differentiation [13,14]. MEG3 is another imprinted lncRNA involved in the regulation of cellular growth, differentiation, and apoptosis. By modulating pathways such as TGF-β/Smad, Wnt/β-catenin, and Notch, MEG3 contributes to neuronal differentiation and increases the expression of genes associated with the neural phenotype, such as Nestin and MAP2 [15,16].

Considering the potential role of exosomal lncRNA cargo in neural differentiation, this study was designed to isolate and characterize NSCs-Exo, investigate their H19 and MEG3 lncRNA content, and evaluate the role of these exosomes in the differentiation of adipose-derived mesenchymal stem cells (ADMSCs) into neuronal-like cells (NLCs).

Materials and Methods

All experimental protocols were approved by the Animal Ethics Committee of Shahid Chamran University (Approval No. IR.SCU.RES.1403.071), and all methods were performed in accordance with the relevant guidelines and regulations.

Isolation of NSCs from the brain

Primary NSCs were isolated in-house from the brains of 1-day-old neonatal Wistar rats purchased from the Laboratory Animal Facility of Shahid Chamran University of Ahvaz, Ahvaz, Iran. All procedures for isolation and culture were performed under completely sterile conditions in a Class II laminar flow hood (Kavosh Mega, Iran). Neonatal rats were anesthetized by intraperitoneal injection of ketamine (100 mg/kg) and xylazine (10 mg/kg) and then rapidly euthanized by decapitation using a sharp surgical blade by trained personnel. Death was confirmed by cessation of heartbeat and respiration and absence of reflexes. Following anesthesia, the skull was opened and the entire brain was removed. The extracted brain tissue was immediately transferred into phosphate-buffered saline (PBS; Sigma, USA) containing 3% penicillin/streptomycin. The cerebral cortex was then isolated and minced into approximately 1 × 1 mm pieces. Enzymatic digestion was performed using trypsin (Gibco, USA). Following digestion, DMEM/F12 (Gibco, USA) supplemented with 10% fetal bovine serum (FBS; Gibco, USA) was added. The samples were then centrifuged at 3000 rpm for 5 min (Armaghan Teb, Iran), passed through 70- and 40-μm cell strainers, and transferred into T25 flasks (SPL, Korea). After 24 h of incubation, the suspended culture medium was transferred to T75 flasks containing 10 mL of DMEM/F12 supplemented with 15% FBS, 1% penicillin/streptomycin, and 20 ng/mL basic fibroblast growth factor (bFGF; Sigma, USA). The flasks were maintained under standard incubation conditions at 37°C and 5% CO_2 (Sina Iran incubator, Iran), and the culture medium was replaced every 3 days. This procedure was continued until the cells reached approximately 70% confluence. To assess neurosphere formation capacity, 10^6 NSCs were cultured under suspension conditions in bacterial culture dishes (SPL, Korea) for 2–4 days. The formation of cellular aggregates was examined using an inverted microscope (Olympus, Japan), and the NSC identity was confirmed by immunocytochemistry for the neural markers Nestin and Sox2[17,18] .

Isolation of exosomes from NSCs

After the cells reached the third passage, the FBS concentration was gradually reduced until the culture medium became serum-free. Following 72 h of incubation under serum-free conditions, the culture supernatant was collected. Exosomes were isolated and purified from the supernatant using a refrigerated centrifuge (GS-1RST, Iran) and the AnaCell Exosome Isolation Kit (Supernatants; AnaCell, Iran).

Initially, the collected culture supernatant was centrifuged at 3000 rpm for 10 min at 4°C to remove cellular debris and larger particles. The supernatant was then passed through a 0.22 µm syringe filter (BSS Fact Bio, Korea) to remove remaining cellular particles. According to the manufacturer's instructions, solution A was added to the samples at a volume ratio of 1:5 (one volume of solution A to five volumes of supernatant). The mixture was thoroughly vortexed and incubated for 12 h at 4°C. Following incubation, the samples were vortexed for 1 min for homogenization and then centrifuged at 800 g for 40 min at 4°C. Finally, 50 µL of solution B was added to the pellet, and the samples were gently mixed [19,20].

Determination of exosome size by dynamic light scattering

The size of the exosomes was determined by dynamic light scattering (DLS) using a Zetasizer Nano ZS (USA). Approximately 200 µL of cell-derived exosomes was suspended in approximately 1.5 mL of pure distilled water. The prepared samples were then transferred to the DLS instrument, and the hydrodynamic diameter of the exosomes was measured.

Morphological evaluation of exosomes by FESEM

To evaluate the morphology of the exosomes, 20 µL of the exosome suspension was placed on a foil surface. After drying with methanol, the sample was gradually dehydrated using methanol

concentrations ranging from 30% to 100%. The sample was then coated with a 2–5 nm layer of gold and imaged using field-emission scanning electron microscopy (FESEM; Mira III TESCAN, Brno, Czech Republic) at an accelerating voltage of 10.0 kV.

Identification of exosomes by transmission electron microscopy

Transmission electron microscopy (TEM) with negative staining using uranyl acetate was employed to evaluate the morphological characteristics of NSCs-Exo. For exosome sample preparation, 300-mesh copper grids coated with Formvar/Carbon were used.

Determination of exosomal protein concentration by Bradford assay

The Bradford assay was used to determine the protein concentration of the isolated exosomes. For each sample, 10 µL of the exosome-containing solution was used. Bradford reagent was added at twice the sample volume; therefore, 10 µL of each exosome sample was added to a well, followed by 20 µL of Bradford reagent. Subsequently, 140 µL of distilled water was added to each well, and the resulting mixture was thoroughly pipetted.

X = Absorbance measured by the instrument – BLANK

$$\frac{X-0/0143}{0/0942} \times Y = \text{Protein concentration (µg/mL)}$$

Y was set to 100 for a sample volume of 10 µL and to 50 for a sample volume of 50 µL.

Detection of exosomal-specific markers by western blotting

To identify and confirm the presence of exosome-specific markers, Western blotting was performed. First, total protein was extracted from the isolated exosomes using an appropriate lysis buffer. A specified amount of protein based on the BCA assay results was loaded onto an SDS-

polyacrylamide gel and electrophoresed. Following separation, the proteins were transferred onto a PVDF membrane.

To prevent nonspecific binding, the membrane was blocked for 1 h in a blocking solution containing 5% non-fat dry milk or BSA in TBST. The membrane was then incubated overnight at 4°C with primary antibodies specific for the exosomal markers CD9, CD63, and CD81 at appropriate dilutions. Following washing with TBST, the membrane was incubated with an HRP-conjugated secondary antibody for 1 h at room temperature. Finally, protein bands were detected using an enhanced chemiluminescence (ECL) solution, and the resulting images were recorded.

RNA extraction from exosomes and evaluation of H19 and MEG3 content

Exosome collection and extraction were continuously performed for one month to obtain a high concentration of exosomes. RNA extracted from the exosomes (by Trizol) was used for cDNA synthesis (by SinaClon kit, Iran). Subsequently, real-time PCR using SYBR Green (Ampicillin kit) was performed to determine the expression of the target genes. The primers are listed in Table 1.

Isolation and culture of adipose-derived mesenchymal

ّtem cells from rat tissue Adipose-derived mesenchymal stem cells (ADMSCs) were isolated in-house from Wistar rats aged 6–8 weeks (200–300 g) purchased from the Laboratory Animal Facility of Shahid Chamran University of Ahvaz, Ahvaz, Iran, as previously described by Hoveizi et al. [20]. Briefly, at the study endpoint, adult rats were euthanized by intraperitoneal (IP) overdose of ketamine (200 mg/kg) and xylazine (20 mg/kg), followed by cervical dislocation as a secondary physical method to ensure death. Death was confirmed by cessation of respiration and heartbeat for >10 min and absence of pedal and corneal reflexes. Under sterile conditions, adipose tissue was harvested from subcutaneous regions of the lower abdomen, perirenal area, and groin. The

tissue was digested with 0.1% collagenase type I for 30 min in a shaker incubator. The resulting suspension was filtered through a 100-µm nylon filter and centrifuged at 3,000 rpm for 8 min. The cell pellet was resuspended in DMEM supplemented with 10% FBS and incubated at 37°C with 5% CO_2 and 98% humidity for 24 h, after which the medium was replaced.

Cellular uptake of exosomes

Exosomes purified in the previous step were tagged with the lipophilic fluorescent probe DiI (Sigma, USA; 1 µM) through a 30-min staining procedure. Free unbound dye was then eliminated by high-speed centrifugation (1000×g, 40 min). Subsequently, ADMSCs were co-cultured with the fluorescently-tagged vesicles for 24 h to allow cellular entry. Internalization was finally visualized under an Olympus BX51 fluorescence microscope (Japan). Exosomes without fluorescent labeling were applied to parallel cultures as the negative control [21].

Treatment of ADMSCs with NSCs-Exo

For differentiation experiments, the cells were cultured in 6- and 24-well plates and maintained in basal culture medium for 24 h. After this period, the basal culture medium was replaced with differentiation medium containing exosomes at a concentration of 10 µg/mL. The neural differentiation medium consisted of DMEM/F12 supplemented with 5% FBS and 1% penicillin/streptomycin. The cells were cultured under these conditions for 14 days, and the culture medium was replaced every 48 h.

Real-time PCR after neural differentiation

To quantitatively evaluate the effect of exosomes on the neural differentiation of MSCs, the expression of the neural markers Nestin, MAP2, Tuj-1, and NF was assessed on day 14 of differentiation using real-time PCR (Roche, Switzerland).

The cells were cultured in 6-well plates at a density of 1×10^5 cells per well. After 24 h, the basal culture medium was replaced with differentiation medium containing exosomes. Following removal of the differentiation medium and washing of the wells with PBS, the cells were lysed with 1 mL of Trizol. The lysate was transferred to a microtube, followed by the addition of chloroform and vortexing. After centrifugation, the aqueous phase containing RNA was collected. RNA was then precipitated using cold isopropanol, washed with 70% ethanol, and dissolved in DEPC-treated water.

RNA concentration and quality were assessed using a NanoDrop One spectrophotometer (Thermo Scientific, USA) at wavelengths of 260 and 280 nm. cDNA synthesis was performed using buffer and enzyme mixes at 47°C, and the samples were stored at −80°C. Real-time PCR was subsequently performed using 1.5 µL of cDNA, specific primers listed in Table 1, and master mix. The reaction consisted of 40 cycles at 95°C, 60°C, and 72°C. Relative gene expression was calculated using the ΔΔCt method, with GAPDH used as the internal control gene.

Table 1. Specific primers used for real-time PCR

Gene/lncRNA	**Primer**	**Sequence (5′–3′)**	**Annealing temperature (°C)**
Tuj-1	F	CAATTTCATCTTTGGTCAGAGTGG	54
	R	TAGGTCTCATCCGTGTTCTCC	54
Nestin	F	AAAGTTCCAGCTGGCTGTGG	55

	R	TCCAGCTTGGGGTCCTGAAA	55
MAP2	F	GCTCTGCCTTTAGCAGC	55
	R	GCTTCTCTGACTCCTTTTCC	55
NF	F	CAGAGCTGGAGGCACTGAAA	58
	R	TCCGAGACACCGATCACTGC	55
H19	F	GGCAGGTGGGGCAGAATGAAT	55
	R	GGGTCAGCGCAGTTCATCAGT	57
MEG3	F	AAATCCTTCCACAGCCACGGG	57
	R	CTGCTGAATGGCTTCCTGGT	58
GAPDH	F	CTGGAGAAACCTGCCAAGTA	58

Immunocytochemistry

To qualitatively evaluate neural differentiation, the expression of neural-specific proteins, including MAP2, Tuj-1, and Nestin, was assessed by immunocytochemistry (ICC). The cells were seeded at a density of 5×10^4 cells per well in 24-well plates. After 24 h, the culture medium was replaced with differentiation medium containing exosomes.

On day 14 of differentiation, the cells were fixed with 4% paraformaldehyde (Sigma, USA), permeabilized with Triton X-100, and blocked with 5% goat serum. The cells were then incubated overnight at 4°C with primary antibodies against MAP2 (1:200, Abcam), Tuj-1 (1:100, Abcam), and Nestin (1:100, Abcam). After washing, the secondary antibody (mouse anti-goat IgG-PE, 1:200) was added and incubated for 3 h at room temperature in the dark. Finally, nuclear staining

was performed using DAPI (Sigma, USA), and the samples were examined and imaged using a fluorescence microscope (Olympus, Japan).

Statistical analysis

All quantitative data are expressed as mean ± standard deviation (SD). Each experiment was performed in triplicate independently (n = 3). Statistical differences among multiple groups were analyzed by one-way analysis of variance (ANOVA) followed by Tukey's post-hoc test using Excel and GraphPad Prism software (version X, USA). A p-value < 0.05 was considered statistically significant.

Results

Isolation and identification of NSCs

Microscopic images showed that NSCs exhibited a polygonal morphology, short dendritic branches, relatively large and bright nuclei, dense cellular aggregates with spherical structures, and high self-renewal capacity during the early stages of culture. Fluorescence microscopy demonstrated the expression of the Nestin and Sox2 markers in neurosphere, which were observed as green fluorescence. Nuclear staining with DAPI uniformly identified the cell nuclei (Fig. 1).

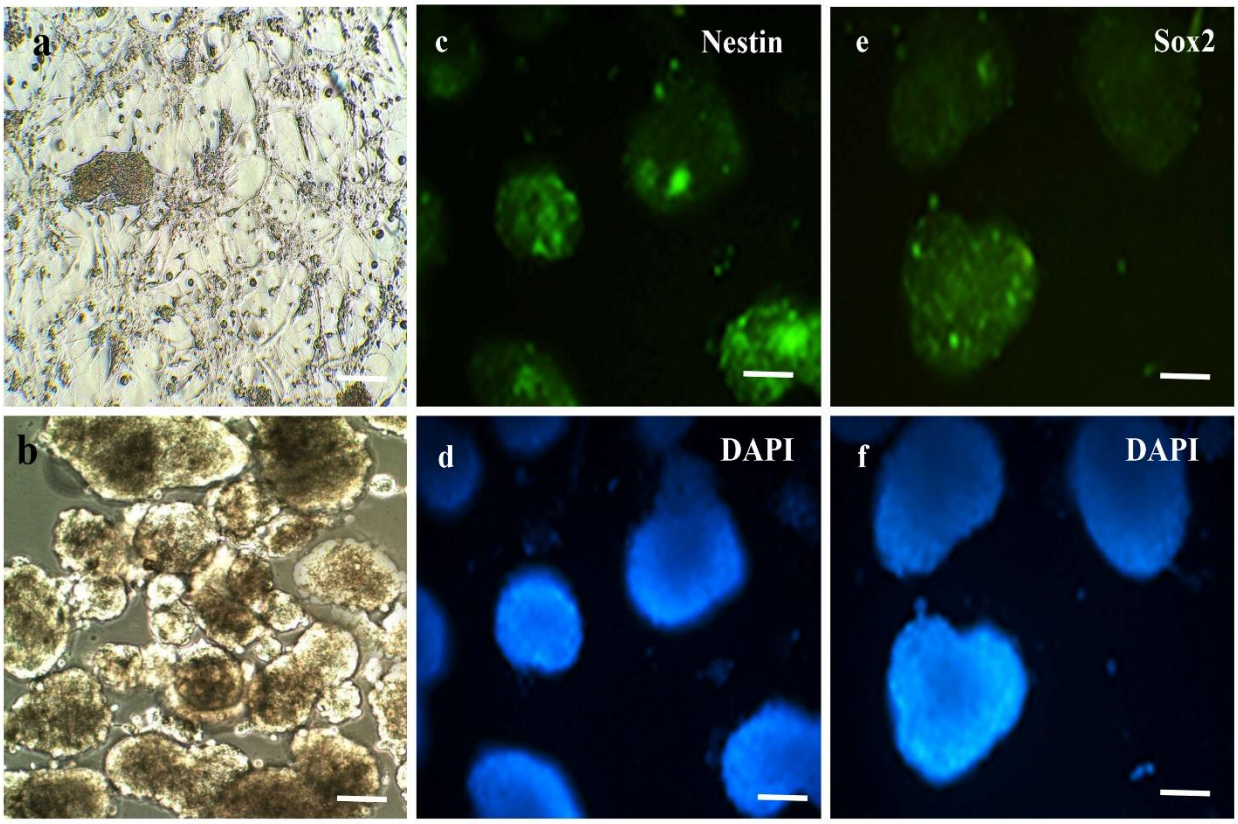


Fig 1. Microscopic images of NSCs. (a) Microscopic image of NSCs isolated from the rat brain using an inverted microscope. (b) Formation of neurospheres from NSCs isolated from the rat brain. (c) Assessment of Nestin marker expression in NSCs using immunocytochemistry (ICC). (d) Corresponding fluorescence image of (c), showing cell nuclei stained with DAPI. (e) Assessment of the neural marker Sox2 expression in NSCs using ICC. (f) Corresponding fluorescence image of (e), showing cell nuclei stained with DAPI.

Identification and characterization of NSCs-Exo

SEM images showed that the isolated particles were predominantly spherical, with a bilayer membrane and a darker central region, indicating a cup-shaped appearance. At lower

magnification, nanoscale particles with a relatively uniform distribution were observed. At higher magnification, the spherical structure of the particles, with clearly defined boundaries and a relatively smooth surface, was readily distinguishable (Fig. 2a-b).

TEM images for the identification of Exo-NSCs

TEM images demonstrated the presence of spherical vesicles with distinct bilayer membranes and nanoscale dimensions (Fig. 2c).

Assessment of specific markers

Western blot analysis demonstrated clear bands corresponding to the exosomal markers CD63, CD81, and CD9 in the exosome samples (Fig. 2d).

Exosomal particle size determined by DLS

DLS analysis showed that the isolated exosomes had a relatively uniform size distribution, with the highest frequency of particles observed within the 30–100 nm range and a mean diameter of 53 nm (Fig. 2e).

Total exosomal protein concentration

The total protein concentration of the isolated exosomes, determined using the Bradford assay, was 330.52 μg/mL.

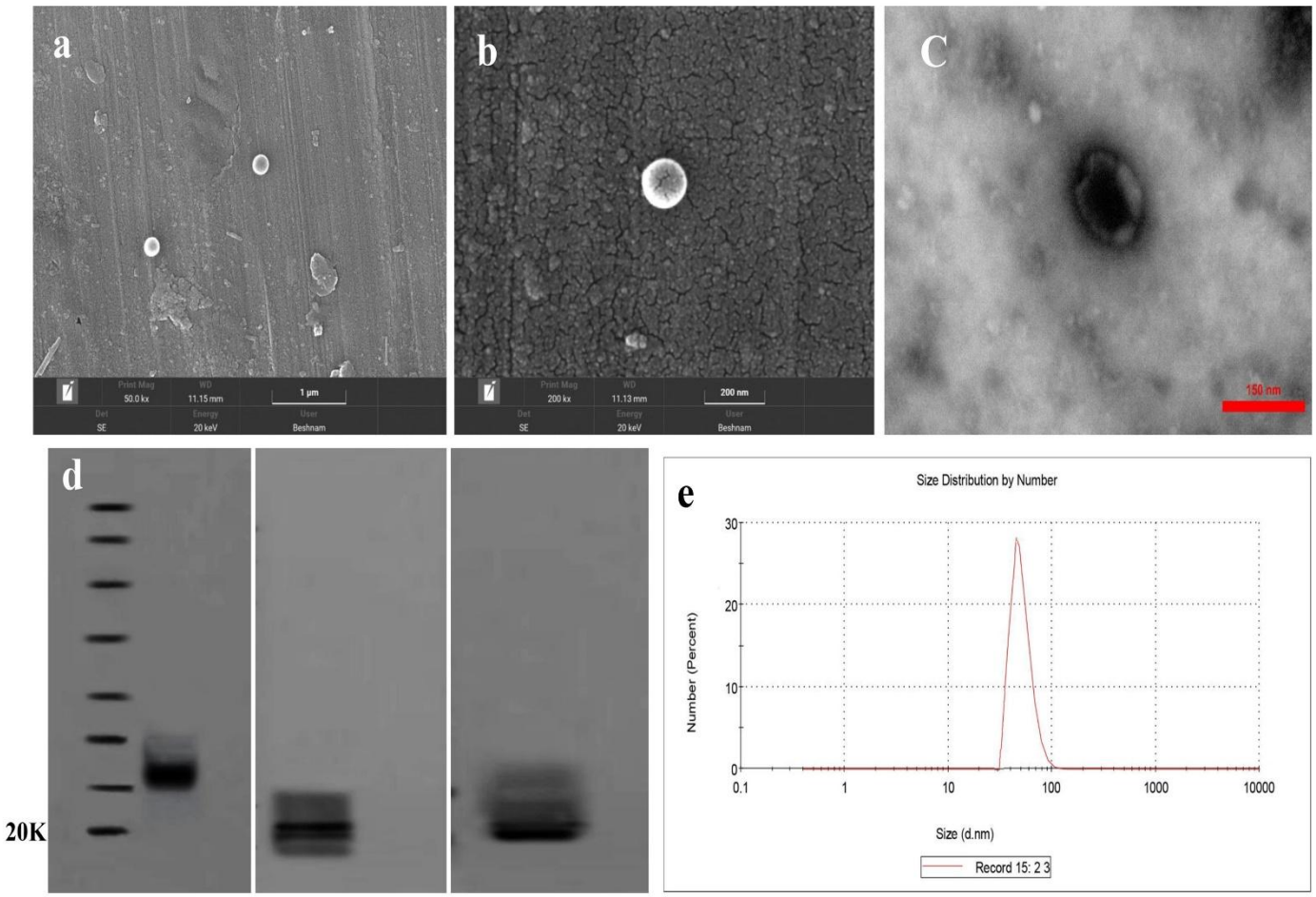
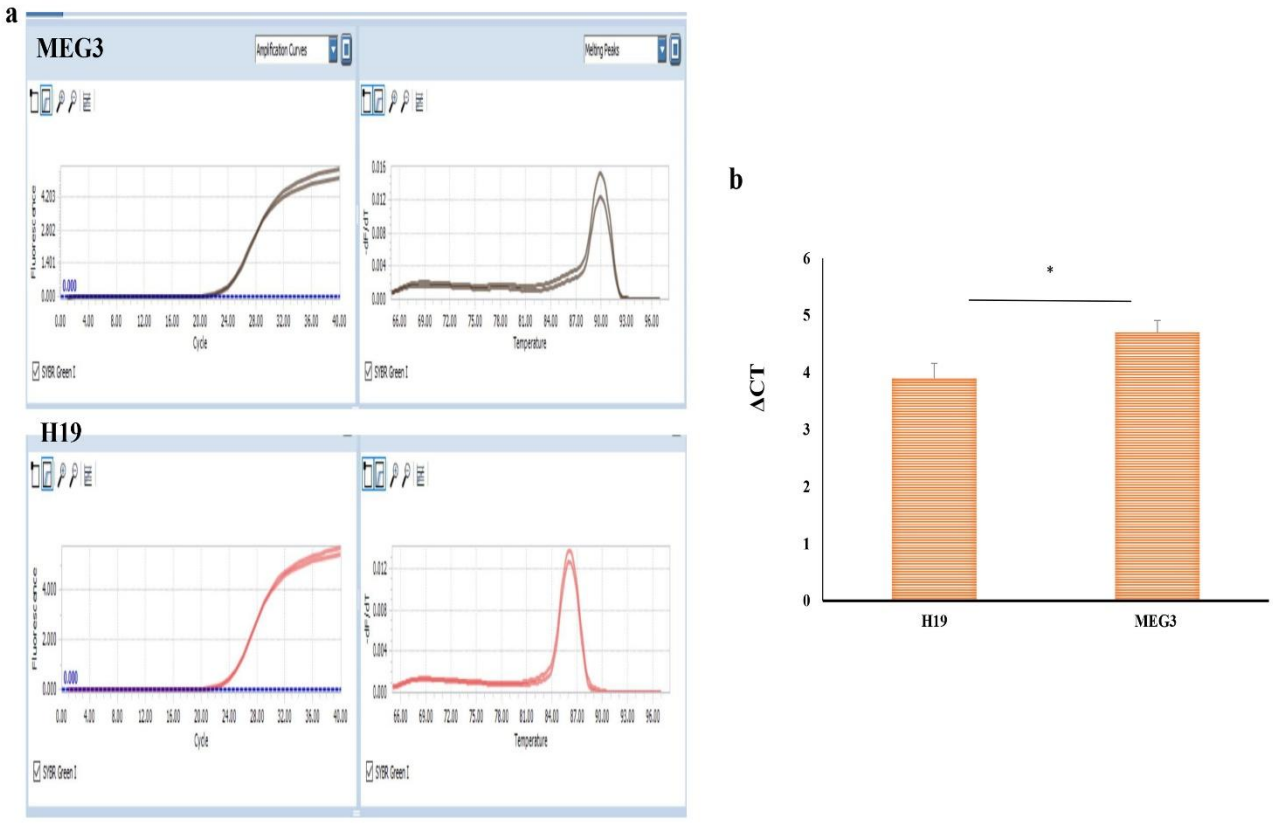


Fig 2. Identification and characterization of NSCs-Exo. (a) SEM images of NSCs-Exo showing predominantly spherical particles with a relatively uniform distribution. (b) SEM image of an individual exosome showing a spherical structure within the nanoscale range. (c) TEM image of isolated exosomes showing spherical vesicular structures with bilayer membranes. (d) Western blot analysis of the exosomal markers CD63, CD81, and CD9. (e) DLS analysis of exosomal particle-size distribution.

Expression of H19 and MEG3 lncRNAs in NSCs-Exo

qRT-PCR results demonstrated that the expression of the H19 and MEG3 lncRNAs was clearly detectable in NSCs-Exo. The amplification curves for both genes showed a gradual and uniform increase in fluorescence signal throughout the qRT-PCR cycles, confirming successful and detectable amplification of these lncRNAs. The melting-curve analysis for both H19 and MEG3 showed a single distinct peak, indicating primer specificity and the absence of nonspecific products or primer-dimer formation (Fig. 3a). Quantitative analysis of the ΔCt values demonstrated that the ΔCt value for H19 was significantly lower than that for MEG3 ($p= 0.023$, $P \leq 0.05$), indicating a higher relative abundance of H19 in the isolated exosomes (Fig. 3b). The data are presented as



mean ± standard deviation, and the observed differences were evaluated using an independent t-test.

Fig 3. qRT-PCR analysis of H19 and MEG3 lncRNA expression in NSCs-Exo. (a) qRT-PCR results showing the amplification curves and melting-curve analysis of H19 and MEG3 in NSCs-Exo. (b) Bar graph showing ΔCt values representing the expression levels of the two lncRNAs in the exosomal cargo. A significant difference in expression levels ($p= 0.023$, $P \leq 0.05$) is indicated by an asterisk (*). Each experiment was repeated at least three times. GAPDH was used for normalization.

Uptake of exosomes by ADMSCs

Fluorescence microscopy images demonstrated that DiI-labeled NSCs-Exo were able to cross the MSC membrane and enter the cytoplasm of these cells (Fig. 4a-b). DiI is a lipophilic dye capable of staining cell membranes. Since the exosomal membrane is derived from the membrane of the source cell, DiI can label the exosomal membrane (Fig. 4c). The accumulation of DiI-labeled exosomes within the cytoplasm of cultured cells indicated their uptake by the cells.

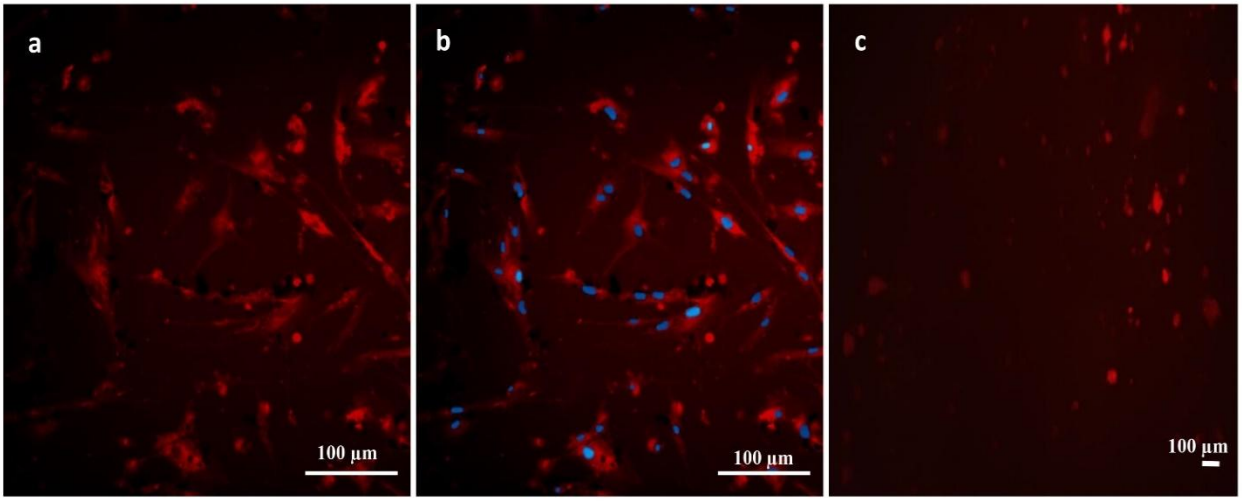


Fig 4. Fluorescence imaging of NSCs-Exo uptake by ADMSCs**.** (a) Red fluorescence in the cytoplasm indicates exosome uptake by the cells. (b) DAPI-stained nuclei merged with the corresponding image. (c) DiI-labeled NSCs-Exo.

Expression of neural markers in NLCs by immunocytochemistry

Figure 5a shows cells that were positive for the neural markers Nestin, MAP2, and Tuj-1. Comparison with the control group indicated that differentiated cells exhibited the characteristic expression of neural-specific markers, whereas such expression was not observed in the control group.

Quantitative analysis of ICC staining demonstrated a significant increase in the percentage of cells positive for the neural markers Nestin, Tuj-1, and MAP2 in the differentiated group ($P \leq 0.001$). According to the graph, approximately 80% of cells were positive for Nestin, 87% for MAP2, and 78% for Tuj-1 in the differentiated group, whereas the percentage of marker-positive cells in the control group was very low (<5%). These increases were statistically significant for all markers and were consistent with the qualitative ICC observations (Fig. 5b).

Expression of neural markers in differentiated cells by qRT-PCR

qRT-PCR results showed a significant increase in the expression of the neural markers Nestin, MAP2, Tuj-1, and NF in differentiated cells after 14 days compared with the control group ($P \leq 0.001$). The relative expression levels of Nestin, MAP2, Tuj-1, and NF were significantly increased compared to the control group, in which the expression of these genes remained at basal levels. These findings demonstrated a marked increase in the expression of neural markers in the differentiated cells (Fig. 5c).

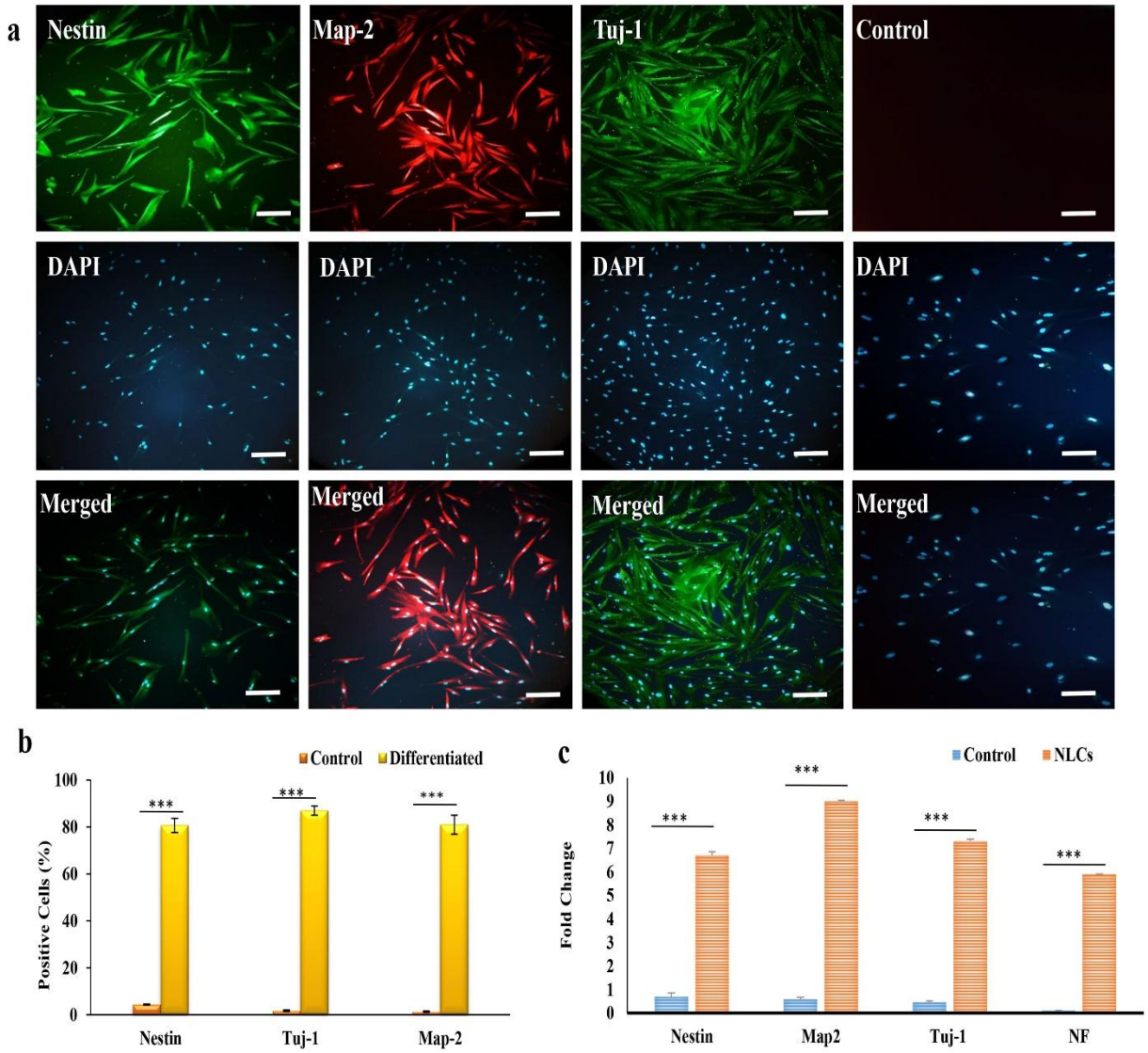


Fig 5. Expression of neural markers in differentiated cells. (a) ICC staining of NLCs for neural markers 14 days after differentiation with NSCs-Exo. Nuclei were stained with DAPI. (b) Quantitative ICC analysis of Nestin, Tuj-1, and MAP2 expression compared with the control group (***P ≤ 0.001). (c) qRT-PCR results showing the expression of Nestin (p= 0.0000012), MAP2 (p= 0.0000002), Tuj-1 (p= 0.0000025), and NF (p= 0.0000001) compared with the control group 14 days after treatment. Each experiment was repeated at least three times. GAPDH was used for normalization. All genes showed statistically significant upregulation (***P ≤ 0.001).

Discussion

The present study investigated the role of NSCs-Exo in the induction of neural differentiation in ADMSCs. Unlike approaches based on direct stem cell transplantation, which are associated with limitations such as low cell survival, the risk of unwanted differentiation, and immune responses, exosomes are extracellular nanovesicles capable of mediating many of the regulatory effects of stem cells through the targeted transfer of biomolecules. These vesicles carry a rich collection of miRNAs, lncRNAs, and proteins and play an important role in intercellular communication and the reprogramming of signaling pathways in recipient cells [1,2].

In this context, Alvarez-Erviti et al. (2011) demonstrated that exosomes derived from mouse dendritic cells can serve as targeted and non-immunogenic carriers for the delivery of therapeutic RNAs to neural cells [22]. Similarly, Takeda and Xu (2015) reported that exosomes derived from differentiating PC12 cells could direct human MSCs toward a neuronal phenotype, accompanied by increased MAP2 and Nestin expression and transfer of miR-125b [23].

In the present study, NSCs-Exo were successfully isolated and characterized. SEM and TEM results confirmed the presence of predominantly spherical vesicles with bilayer membranes and sizes mainly ranging from 30 to 100 nm, with a mean diameter of 53 nm. Confirmation of the expression of the specific exosomal markers CD63, CD81, and CD9 by Western blotting further supported the exosomal identity of the isolated particles. These observations are consistent with the findings of Yuan et al. (2021), who characterized exosomes using TEM, NTA, and the markers CD9 and Flotillin-1 [4].

One of the main objectives of this study was to investigate the presence of H19 and MEG3 lncRNAs within NSCs-Exo. qRT-PCR results, characterized by uniform amplification curves and distinct melting peaks, confirmed the detectable presence of both lncRNAs in NSCs-Exo. This finding is important because, although the role of lncRNAs in the regulation of neural differentiation has increasingly been recognized, their transfer through exosomes derived from neural stem cells as potential mediators of differentiation has received comparatively less attention. Kalluri (2020) demonstrated that exosomes can transfer lncRNAs between cells [3]; the present study extends this concept to the context of neural differentiation of ADMSCs and provides additional experimental evidence for this potential mechanism.

The next stage of the study was to confirm the uptake of NSCs-Exo by target cells. Fluorescence microscopy demonstrated the successful uptake of DiI-labeled NSCs-Exo into the cytoplasm of ADMSCs. This finding provides evidence supporting the cellular entry of exosomes and serves as a basis for interpreting their potential differentiation-related effects.

The most important functional finding of this study was the induction of neural differentiation in ADMSCs following treatment with NSCs-Exo. The immunocytochemistry and qRT-PCR results consistently demonstrated successful neural differentiation of ADMSCs after 14 days of treatment.

ICC analysis showed significant expression of Nestin, Tuj-1, and MAP2 in the treated group, whereas the control group showed minimal expression (<5%). The percentages of positive cells in the differentiated group were approximately 80% for Nestin, 87% for MAP2, and 78% for Tuj-1. This expression pattern is consistent with the progressive nature of neuronal differentiation, with Nestin representing an early neural marker and Tuj-1 and MAP2 representing markers associated with later stages of neuronal differentiation and maturation. The simultaneous increase in these markers suggests progression along the differentiation pathway from early neural stages toward neuronal maturation [24,25].

The qRT-PCR results further supported this pattern, showing approximately threefold, fourfold, 3/2-fold, and twofold increases in Nestin, MAP2, Tuj-1, and NF expression, respectively, compared with the control group, in which these expression levels were below 1. The agreement between the qualitative ICC findings and quantitative qRT-PCR results strengthens the validity of the observations and suggests that exosome treatment was associated with changes in gene expression at the transcriptional level rather than merely transient morphological alterations.

These findings are consistent with previous studies investigating the role of exosomes in neural differentiation. Yuan et al. (2021) reported that NSCs-Exo could direct target cells toward a neuronal phenotype and attributed this effect primarily to the transfer of miR-9 and inhibition of Hes1 [4]. However, the present study differs from previous approaches in two main respects. First, rather than focusing on a single miRNA, this study investigated the presence of two regulatory upstream lncRNAs, H19 and MEG3, within the exosomal cargo and emphasized their potential capacity to regulate multiple signaling pathways simultaneously through mechanisms such as ceRNA interactions and interactions with miRNAs. Second, the target cells in the present study were ADMSCs, which are of particular interest for regenerative medicine because of their

accessibility and high proliferative capacity, making them a potentially valuable cellular source for clinical applications.

Within this context, the role of the H19 lncRNA in neurogenesis following stroke was reported by Fan et al. [26]. Although that study focused on intracellular H19 expression under neurogenic conditions, it demonstrated that increased H19 expression was associated with enhanced neural differentiation, complementing the present observations regarding the presence and potential role of H19 in neural differentiation. Similarly, several studies have reported a role for MEG3 in regulating neural cell fate through modulation of related signaling pathways [26]. Collectively, the findings of the present study, together with these previous observations, suggest that the simultaneous transfer of H19 and MEG3 by neural stem cell-derived exosomes may provide an effective molecular basis for the induction of neural differentiation in ADMSCs.

Several limitations of the present study should be considered when interpreting the findings. First, the study was conducted exclusively under *in vitro* conditions. Although cell culture models are useful for investigating the molecular mechanisms of neural differentiation, they cannot fully reproduce the complexity of the *in vivo* nervous system. Cellular interactions, microenvironmental factors, and tissue-derived signals present in vivo may influence cell behavior and exosome function. Second, the downstream molecular mechanisms of H19 and MEG3 were not functionally investigated. Although the presence of these lncRNAs was observed concurrently with increased expression of neural markers, the precise signaling pathways and target miRNAs involved in this process were not confirmed through knockdown or overexpression experiments. Therefore, the observed relationships should primarily be interpreted at the level of gene-expression association, and additional functional interference studies will be necessary to establish causality for H19 and MEG3.

Despite these limitations, the present findings are valuable from two perspectives. First, the study demonstrated the potential of exosomes to induce neural differentiation in ADMSCs without the need for direct genetic manipulation, representing an approach with potential practical advantages for future clinical applications. Second, the simultaneous presence of two upstream regulatory lncRNAs within the exosomal cargo supports the concept that neural stem cell-derived exosomes may provide a multilayered platform for the transfer of differentiation-related signals that extends beyond the action of individual miRNAs.

Conclusion

The present study demonstrated that NSCs-Exo contain the lncRNAs H19 and MEG3 and can be taken up by adipose-derived mesenchymal stem cells. Treatment of ADMSCs with NSCs-Exo was associated with increased expression of neural markers, including Nestin, MAP2, Tuj-1, and NF, as demonstrated by immunocytochemistry and qRT-PCR after 14 days of treatment. These findings suggest that NSCs-Exo may contribute to the acquisition of a neuronal-like phenotype in ADMSCs and highlight their potential as a cell-free approach for neural regeneration and regenerative medicine.

Declaration of competing interest

The authors affirm that they have no potential conflicts of interest to disclose.

Data availability

Data will be made attainable on request.

Acknowledgements

The authors are grateful to Shahid Chamran University of Ahvaz for funding this study.

Author Contribution

Y.H: carried out the experiment and wrote the manuscript, E.H: designed and directed the project, M.N: contributed to data and interpretation of data. All authors have read and approved the final manuscript.

Funding

This study was funded and supported by the Shahid Chamran University of Ahvaz (Grant Number: SCU.SB1404.12464).

Declarations

Ethics approval: The animal experiment was approved by the Animal Ethics Committee of Shahid Chamran University (Approval No. IR.SCU.RES.1403.071). All methods were performed in accordance with the relevant guidelines and regulations.

Consent to Participate

Not applicable.

Consent for Publication

Not applicable

Conflict of Interests

No conflict or competing financial interests exist.

References

1 Alammari, F., Al-Hujaily, E. M., Alshareeda, A., Albarakati, N. & Al-Sowayan, B. S. Hidden regulators: the emerging roles of lncRNAs in brain development and disease. *Frontiers in neuroscience* **18**, 1392688 (2024).

2 Llorente, V., Velarde, P., Desco, M. & Gómez-Gaviro, M. V. Current understanding of the neural stem cell niches. *Cells* **11**, 3002 (2022).

3 Kalluri, R. & LeBleu, V. S. (2020).

4 Yuan, P. *et al.* Neural stem cell-derived exosomes regulate neural stem cell differentiation through miR-9-Hes1 axis. *Frontiers in Cell and Developmental Biology* **9**, 601600 (2021).

5 Ramos, A. D. *et al.* Integration of genome-wide approaches identifies lncRNAs of adult neural stem cells and their progeny in vivo. *Cell stem cell* **12**, 616-628 (2013).

6 Jankowski, M. *et al.* Unveiling mesenchymal stem cells' regenerative potential in clinical applications: insights in miRNA and lncRNA implications. *Cells* **12**, 2559 (2023).

7 Zhang, Q. *et al.* The role of exosomes derived from stem cells in nerve regeneration: A contribution to neurological repair. *Experimental Neurology* **380**, 114882 (2024).

8 Liu, W.-z., Ma, Z.-j., Li, J.-r. & Kang, X.-w. Mesenchymal stem cell-derived exosomes: therapeutic opportunities and challenges for spinal cord injury. *Stem cell research & therapy* **12**, 102 (2021).

9 Margiana, R. *et al.* Clinical application of mesenchymal stem cell in regenerative medicine: a narrative review. *Stem cell research & therapy* **13**, 366 (2022).

10 Li, L. *et al.* Transplantation of human mesenchymal stem-cell-derived exosomes immobilized in an adhesive hydrogel for effective treatment of spinal cord injury. *Nano letters* **20**, 4298-4305 (2020).

11 Yang, Y. *et al.* Long non-coding RNA regulation of mesenchymal stem cell homeostasis and differentiation: advances, challenges, and perspectives. *Frontiers in Cell and Developmental Biology* **9**, 711005 (2021).

12 Daneshmoghadam, J. *et al.* The gene expression of long non-coding RNAs (lncRNAs): MEG3 and H19 in adipose tissues from obese women and its association with insulin resistance and obesity indices. *Journal of clinical laboratory analysis* **35**, e23741 (2021).

13 Wang, Y. *et al.* Long noncoding RNA H19: a novel oncogene in liver cancer. *Non-coding RNA* **9**, 19 (2023).

14 Wu, B. *et al.* Long noncoding RNA H19: a novel therapeutic target emerging in oncology via regulating oncogenic signaling pathways. *Frontiers in Cell and Developmental Biology* **9**, 796740 (2021).

15 Li, H. *et al.* The long noncoding RNA H19 promotes fibrotic processes in lens epithelial cells. *Investigative Ophthalmology & Visual Science* **64**, 21-21 (2023).

16 Wang, L. & Qi, L. The role and mechanism of long non-coding RNA H19 in stem cell osteogenic differentiation. *Molecular medicine* **27**, 86 (2021).

17 Karimi, A., Hoveizi, E., Khajehpour, L., Ghotbeddin, Z. & Pyecroft, S. The Effects of Neural Stem Cell-Derived Exosomes in the Improvement of Passive Avoidance Memory: A Behavioral, Molecular, and Electrophysiological Study in Adult Male Wistar Rats. *Journal of Molecular Neuroscience* **76**, 15 (2026).

18 Hoveizi, E., Doraghi, K. & Rostami, E. Fabrication and Characterization of Resveratrol-Loaded Solid Lipid Nanoparticles: Evaluation of Neuroprotective, Neurobehavioral, and Molecular Outcomes. *Molecular neurobiology* **63**, 346 (2026).

19 Hoveizi, E., Karimi, A., Khajehpour, L., Ghotbeddin, Z. & Pyecroft, S. Astrocyte-derived exosomes in cognitive recovery: A comparative assessment of neurobehavioral, molecular, and electrophysiological dimensions. *Behavioural Brain Research*, 116196 (2026).

20 Hoveizi, E. & Sayahi, M. Fabrication and characterization of 3D-printed polyacrylonitrile scaffolds for the neural differentiation of mesenchymal stem cells via exosomes. *Journal of Biological Engineering* **20**, 90 (2026).

21 Haghshenas, M., Hoveizi, E., Mohammadi, T. & Kazemi Nezhad, S. R. Use of embryonic fibroblasts associated with graphene quantum dots for burn wound healing in Wistar rats. *In Vitro Cellular & Developmental Biology-Animal* **55**, 312-322 (2019).

22 Alvarez-Erviti, L. *et al.* Delivery of siRNA to the mouse brain by systemic injection of targeted exosomes. *Nature biotechnology* **29**, 341-345 (2011).

23 Takeda, Y. S. & Xu, Q. Neuronal differentiation of human mesenchymal stem cells using exosomes derived from differentiating neuronal cells. *PloS one* **10**, e0135111 (2015).

24 Hoveizi, E., Bijavi, G. & Parsa, H. Advancing Cell Therapy to Enhance Passive Avoidance Memory: Integrative Approaches Combining Neural-Like Cells and Rosmarinic Acid Through Behavioral, Molecular, and Histological Analyses. *Neurochemical Research* **50**, 334 (2025).

25 Bostani, A., Hoveizi, E., Naddaf, H. & Razeghi, J. Nerve regeneration through differentiation of endometrial-derived mesenchymal stem cells into nerve-like cells using polyacrylonitrile/chitosan conduit and berberine in a rat sciatic nerve injury model. *Molecular neurobiology* **62**, 1493-1510 (2025).

26 Fan, B. *et al.* Long noncoding RNA mediates stroke-induced neurogenesis. *Stem Cells* **38**, 973-985 (2020).